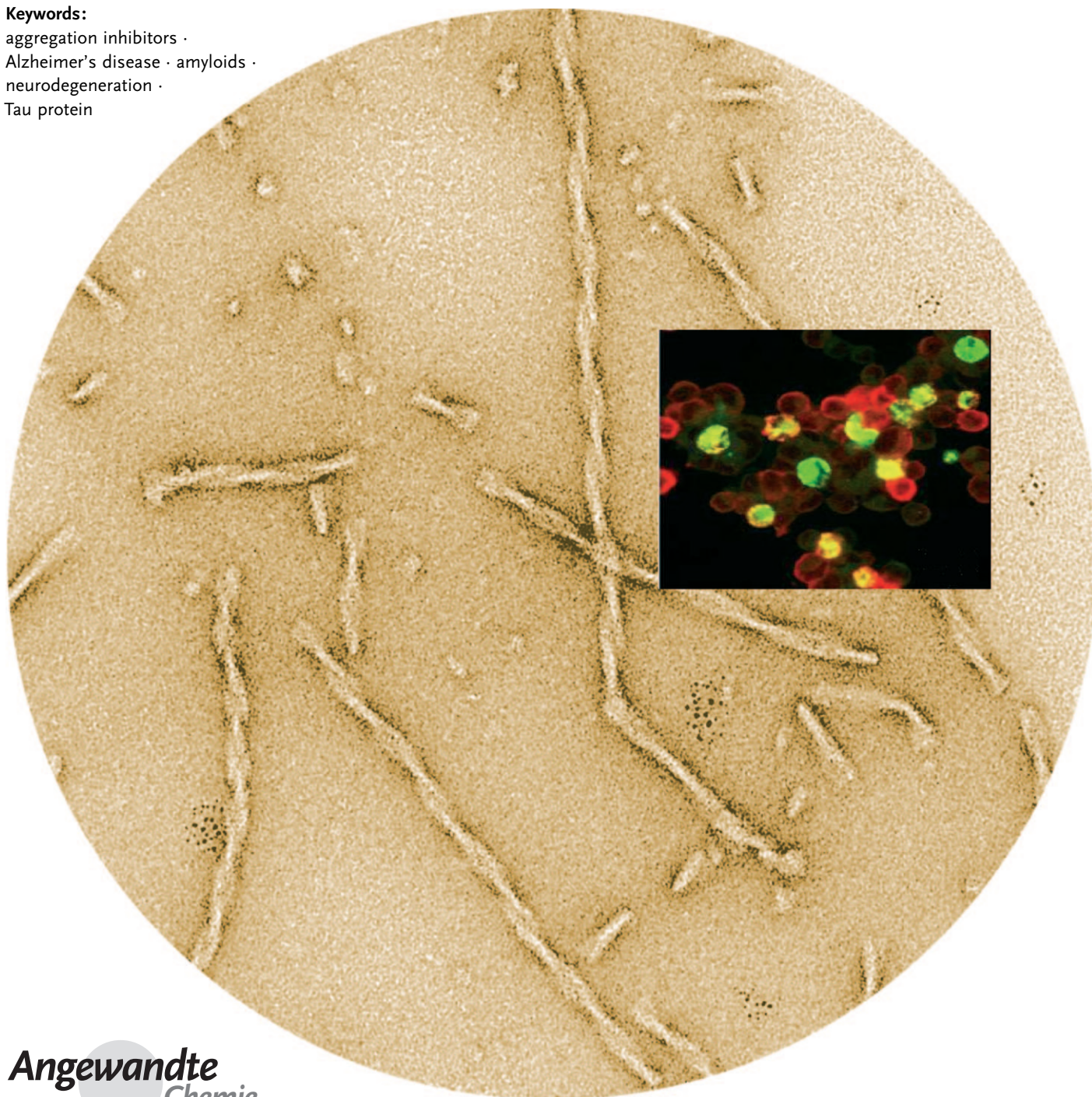


# Development of Tau Aggregation Inhibitors for Alzheimer's Disease

*Bruno Bulic,\* Marcus Pickhardt, Boris Schmidt, Eva-Maria Mandelkow, Herbert Waldmann, and Eckhard Mandelkow\**

**Keywords:**

aggregation inhibitors ·  
Alzheimer's disease · amyloids ·  
neurodegeneration ·  
Tau protein



A variety of human diseases are suspected to be directly linked to protein misfolding. Highly organized protein aggregates, called amyloid fibrils, and aggregation intermediates are observed; these are considered to be mediators of cellular toxicity and thus attract a great deal of attention from investigators. Neurodegenerative pathologies such as Alzheimer's disease account for a major part of these protein misfolding diseases. The last decade has witnessed a renaissance of interest in inhibitors of tau aggregation as potential disease-modifying drugs for Alzheimer's disease and other "tauopathies". The recent report of a phase II clinical trial with the tau aggregation inhibitor MTC could hold promise for the validation of the concept. This Review summarizes the available data concerning small-molecule inhibitors of tau aggregation from a medicinal chemistry point of view.

## 1. Introduction

The search for small-molecule inhibitors of amyloid fibril formation is of fundamental importance for both academic and industrial research. More than one hundred amyloid-related diseases, among them Alzheimer's disease, tauopathies, type II diabetes mellitus, and BSE, are linked to the aggregation of one of twenty nonhomologous human proteins.<sup>[1,2]</sup> Therefore, the scarcity of amyloid aggregation inhibitors that have progressed through clinical trials is unexpected.<sup>[3–6]</sup> The lack of success in this field is not so much the result of decision makers reluctant to pursue unconfirmed targets as a consequence of the complexity of the processes underlying fibril formation and pathogenicity, which lies at the crossroads of biology and physics. Indeed, precise atomic-level structural information of the fibril target is lacking,<sup>[7]</sup> as is a basic understanding of the fibril self-assembly processes. The most straightforward strategy to face this challenge is the screening of compound libraries containing sufficient structural diversity. Identification of hits generally allows subsequent medicinal chemistry efforts to develop compounds displaying the desired properties, that is, optimized inhibitory potencies and pharmacokinetics.

In this Review we primarily address inhibitors of tau aggregation. This type of aggregation is characteristic for "tauopathies", that is, brain diseases in which tau assembles into abnormal fibers ("paired helical filaments", PHFs) that form higher-order aggregates ("neurofibrillary tangles" or "neuropil threads") in neurons or other types of brain cells.<sup>[8–10]</sup> Electron microscopy of PHFs formed by tau was first described by Kidd.<sup>[11]</sup> PHFs are formed by two filaments twisted around one another with a crossover repeat of 80 nm and a width of 8–20 nm. The filaments are formed by tau proteins with a cross- $\beta$ -sheet conformation.<sup>[12,13]</sup>

The most common tauopathy is Alzheimer's disease, but tau deposits also occur in frontotemporal dementias (FTDP-17), Pick's disease, Parkinson's disease, progressive nuclear palsy, and other conditions.<sup>[14,15]</sup> In Alzheimer's disease, the brain contains two types of aggregates: intracellular neurofibrillary tangles (tau protein) and extracellular senile or

## From the Contents

1. Introduction	1741
2. Tau Aggregation Inhibitors	1743
3. Aggregation Inhibitors for Other Amyloidogenic Proteins	1749
4. Binding Mode	1750
5. Summary and Outlook	1750

"amyloid" plaques consisting of the A $\beta$  peptide, a cleavage product of the membrane protein APP.<sup>[16]</sup> Both types of aggregates are toxic for neurons,

and both are based on the principle of amyloid aggregation, in which fibers are formed from the subunit protein by axial stacking of  $\beta$  strands, generating a cross- $\beta$ -sheet structure at the core of the filaments.

Tau protein as such is highly soluble, since it mostly contains hydrophilic residues. Its main role is the stabilization of microtubules in neuronal axons to ensure their function as tracks for axonal transport and as cytoskeletal elements for the growth or branching of axons. In the adult human central nervous system, tau occurs as six main isoforms, ranging from 352 to 441 residues in length, which are generated by alternative splicing of a single gene on chromosome 17. In comparison to other amyloids, tau is unusual in that only a small part of the molecule is involved in the abnormal aggregation process. This part, in particular the one or two "hexapeptide motifs", resides in the "repeat domain" which consists of three or four stretches of approximately 31 imperfectly repeated amino acids (depending on isoform; repeat R2 may be absent owing to alternative splicing; Figure 1).<sup>[17]</sup> Tau is a natively unfolded protein lacking a defined 3D structure; it is hence not amenable to X-ray structure analysis, but the repeat domain has been analyzed by NMR spectroscopy.<sup>[18,19]</sup>

[\*] Dr. B. Bulic, Prof. H. Waldmann  
Max-Planck-Institute for Molecular Physiology, Dortmund  
and  
Center for Applied Chemical Genomics, Dortmund  
E-mail: bruno.bulic@mpi-dortmund.mpg.de  
and  
Technische Universität Dortmund (Germany)  
Fax: (+49) 231-133-2499

Dr. M. Pickhardt, Dr. E.-M. Mandelkow, Prof. E. Mandelkow  
Max-Planck-Unit for Structural Molecular Biology  
c/o DESY, Notkestrasse 85, 22607 Hamburg (Germany)  
Fax: (+49) 8971-6810  
E-mail: mand@mpasmb.desy.de

Prof. B. Schmidt  
Clemens-Schöpfung-Institute for Organic Chemistry and Biochemistry  
Technische Universität Darmstadt  
Petersenstrasse 22, 64287 Darmstadt (Germany)



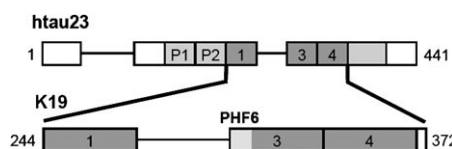


**Figure 1.** Tau isoform and construct used in the PHF inhibition assay. Construct K19 (repeat domain with three repeats, R2 absent).

The exact pathway by which neurons degenerate in Alzheimer's disease is still poorly understood and is subject to intense research. However, there is a general consensus

that protein aggregation is a major element of cell toxicity, and therefore various laboratories are investigating the possibility of inhibiting aggregation by means of small molecules that could be developed into drugs. Two major approaches are distinguishable for tau aggregation: 1) The search for inhibitors of kinases that phosphorylate tau. This approach is based on the assumption that abnormally phosphorylated tau protein aggregates more readily.<sup>[20,21]</sup> 2) The search for direct inhibitors of the tau aggregation process. We will describe the second approach. It is noteworthy that recent data on a phase II clinical trial with the drug candidate MTC support the concept of tau aggregation inhibition as a means to address Alzheimer's disease.<sup>[95]</sup>



Eckhard Mandelkow studied physics in Braunschweig, New Orleans, and Hamburg, and received his Ph.D. at the Max Planck Institute for Medical Research in Heidelberg for research on the X-ray structure analysis of tobacco mosaic virus (with Prof. K. C. Holmes). After a postdoctoral stay at Brandeis University, he completed his habilitation on cytoskeletal structures at the MPI in Heidelberg. In 1986 he became professor at the University of Hamburg and director at the Max Planck Unit for Structural Molecular Biology at DESY, Hamburg.



Marcus Pickhardt was born in Cuxhaven, Germany in 1966. He received his diploma in microbiology from the University Göttingen in the group of Prof. H. G. Schlegel. He joined the group of Prof. R. Thomssen at the Institute of Medicinal Microbiology in Göttingen and received his Ph.D. for the structural analysis of hepatitis C virus surface proteins. Since 2000 he has been a research scientist in the group of Prof. E. Mandelkow at the Max Planck Institute for Structural Molecular Biology, Hamburg. He is interested in the structural properties of the microtubule associate tau protein.



Hebert Waldmann was born in Neuwied, Germany. He studied chemistry at the University of Mainz, where he received his Ph.D. in organic chemistry in 1985 under the guidance of Prof. H. Kunz. After a postdoctoral appointment with Prof. G. Whitesides at Harvard University, he completed his habilitation at the University of Mainz in 1991. He was a professor at the University of Bonn and the University of Karlsruhe before being appointed in 1999 as director of the Max Planck Institute of Molecular Physiology Dortmund and professor of organic chemistry at the University of Dortmund. His research interests lie in the syntheses of signal transduction modulators and natural-product-derived compound libraries, the synthesis of lipidated peptides and proteins, and in protein microarray technology.



Bruno Bulic was born in Paris, France. He received his M.Sc. in chemistry and biochemistry from the University Paris VI while working with Prof. J.-P. Genet. He joined the group of Prof. A. Pfaltz (Basel, Switzerland), where he received his Ph.D. in 2004 for research on palladium- and copper-catalyzed C–C bond formation. He then performed postdoctoral research with Prof. H. Waldmann at the Max Planck Institute of Molecular Physiology Dortmund, where he was appointed group leader in 2006. His research focuses on the development of tau aggregation inhibitors for Alzheimer's disease.



Boris Schmidt, born in Trinidad in 1962, studied chemistry at the University of Hannover and Imperial College in London and obtained his PhD with Prof. H. M. R. Hoffmann in 1991. After research stays at Uppsala University and Scripps Research Institute, La Jolla, he joined Novartis CNS research in 1999 before relocating to Technische Universität Darmstadt in 2002 to focus on the medicinal chemistry of neurodegenerative diseases.



Eva-Maria Mandelkow studied medicine in Heidelberg and Hamburg and received her Ph.D. at the Max Planck Institute for Medical Research, Heidelberg, for research on enzyme kinetics of the motor protein myosin (with Prof. K. C. Holmes). She performed postdoctoral research at Brandeis University and at the Scripps Research Institute in La Jolla. She joined the MPI in Heidelberg as research scientist where she studied the self-assembly of microtubules and cryo-electron microscopy of proteins. In 1986 she became principal investigator at the Max Planck Unit for Structural Molecular Biology at DESY, Hamburg.

## 2. Tau Aggregation Inhibitors

For the tau aggregation assay in the presence of thioflavin S, the tau construct K19 was used, which represents the three-repeat domain of the fetal human isoform hTau23 (Figure 1). This protein aggregates overnight to paired helical filaments (PHFs) with high reproducibility, which makes it appropriate for an automated screening system. The three-repeat tau construct corresponds to the core of the PHF structure and contains the hexapeptide motif VQIVYK, the conversion of which to a  $\beta$ -sheet structure promotes aggregation.<sup>[17]</sup>

A library of 200 000 compounds was screened both for inhibition of tau aggregation and for induced disassembly of tau aggregates,<sup>[22]</sup> an additional feature that is rarely observed among commonly screened compounds (Figure 2). The compound set used for the primary screen was selected according to the Lipinski rules.

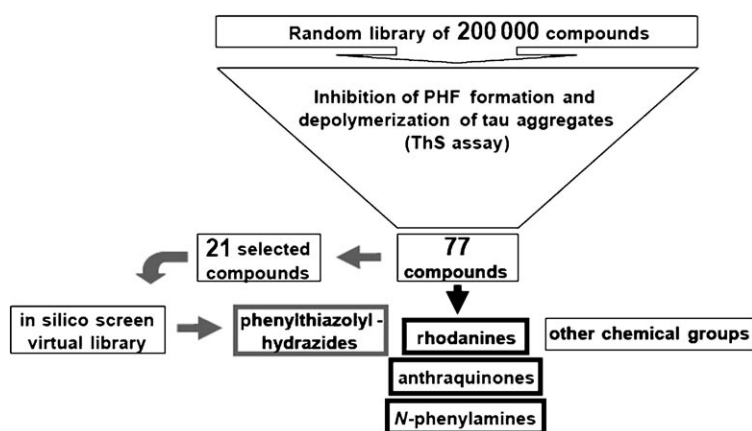


**Figure 2.** Screening scheme leading to the phenylthiazolylhydrazide and rhodanine lead structures. Starting from 200 000 compounds, 77 compounds were identified that were able to inhibit tau aggregation and to dissolve preformed PHFs. The chemical class of rhodanines was identified as one of the active hits. Using 21 of the 77 compounds, an in silico screen was performed from which the phenylthiazolylhydrazides were first identified as a hit.<sup>[23]</sup>

The initial screening for active compounds and validation of the results were accomplished by a thioflavin S fluorescence assay<sup>[24]</sup> in which the emission intensity of thioflavin S fluorescence at 521 nm is greatly increased in the presence of PHFs (excitation at 440 nm). This fluorescence increase is proportional to the extent of aggregation (Figure 3).

The primary screen was described by Pickhardt et al.<sup>[22,25]</sup> The tau protein was incubated overnight under proaggregation conditions in the presence of the screened compound (Figure 4). After addition of thioflavin S, the aggregation was quantified by measurement of the emission at 512 nm (excitation at 440 nm). Typical fluorescence spectra of ThS in the presence of soluble or aggregated protein are shown in Figure 3. The secondary screen (disassembly of preformed tau fibrils) was performed by incubation of PHFs in the presence or absence of compounds overnight at 37 °C, after which the ThS fluorescence of the remaining fibrils was measured. The obtained Z factor of 0.81 confirmed the reliability of the

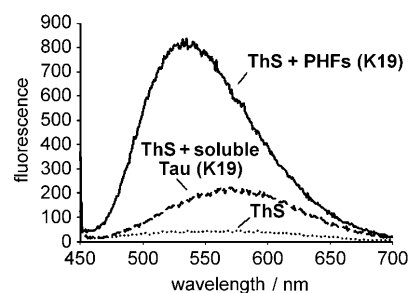


**Figure 3.** Thioflavin S (ThS) fluorescence can be used to measure the aggregation of tau into PHFs

assay.<sup>[26]</sup> The results were verified with other assays (electron microscopy, filter/pelleting assay) as well as with other tau constructs and isoforms.

In general, the properties of phosphorylated tau with regard to detachment from microtubules and aggregation into fibrils depend on its phosphorylation state.<sup>[28]</sup> However, the screening was performed with unphosphorylated recombinant tau, because this protein polymerizes well into paired helical filaments. The similarity of these fibers to those purified from Alzheimer brain tissues has been assessed by electron microscopy and spectroscopic methods, indicating that the in vitro aggregation is a reliable PHF model.<sup>[29]</sup>

In the primary ThS screen, the compounds were tested for their potential self-fluorescence at the given excitation and emission wavelengths. All compounds that showed a higher fluorescence signal in the absence of protein than in its presence were excluded from further testing. To exclude possible effects from quenching or ThS displacement, the substances were also tested in “dye-free” assays, such as pelleting and filter assays, intrinsic tryptophan fluorescence, or electron microscopy.

Of the identified hits, 77 compounds (0.04 % of the library) were able to induce PHF disassembly

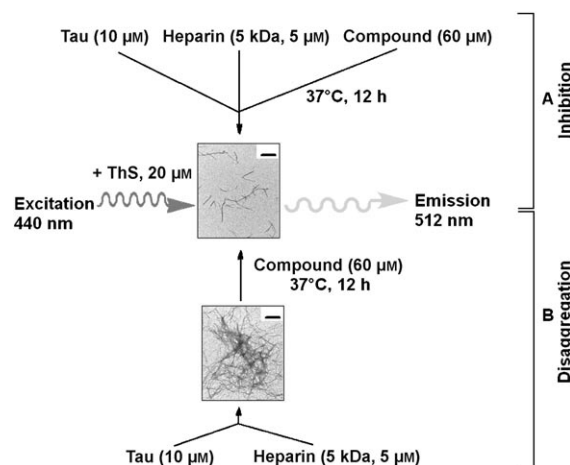


**Figure 4.** Thioflavin S (ThS) fluorescence assay for compounds that inhibit aggregation of tau into PHFs (A) and disaggregate preformed PHFs (B).<sup>[27]</sup> Scale bars in microscopy images: 500 nm.

with 80 % efficiency at 60  $\mu\text{M}$  compound concentration. These hits can be classified into a few clusters according to their chemical structures. Details on the inhibitory activities obtained from the *N*-phenylamines, anthraquinones, phenylthiazolylhydrazides (PTHs), and thioxothiazolidinones (rhodanines) are described elsewhere.<sup>[22,23,27,30,31]</sup>

A preliminary structure–activity relationship (SAR) for the PTH and rhodanine compounds was deduced from in vitro activities of substances obtained in a chemical synthesis program primarily aimed at elucidating the requirements for improved inhibitory potencies. The efficacy of the compounds was subsequently tested on a neuronal cell model of tau aggregation (Figure 5).

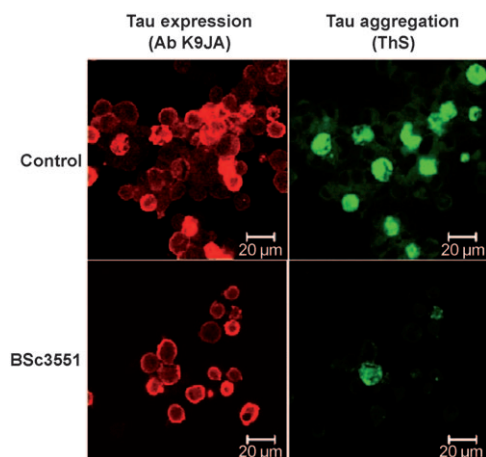


**Figure 5.** Tau expression, aggregation, and inhibition in a cellular model.<sup>[23]</sup>

### 2.1. Rhodanine-Based Inhibitors

The rhodanine-based compounds (Figure 6) are members of an appealing hit class. Although derivatives are suspected to undergo conjugate addition in vivo,<sup>[32]</sup> they are frequently

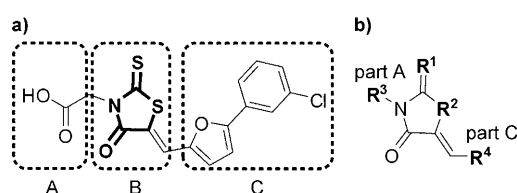


**Figure 6.** Variation of rhodanine inhibitor structure. a) Structure of the hit compound. Variation of regions flanking the central rhodanine core (part B) is possible in parts A and C. b) Illustration of the variations of the core (R<sup>1</sup> and R<sup>2</sup>) and of the flanking substituents (R<sup>3</sup> and R<sup>4</sup>).<sup>[27]</sup>

employed in medicinal chemistry, as there is no adverse effect (e.g. mutagenicity) correlated to this chemical structure. According to a long-term clinical study with epalrestat, an aldose reductase inhibitor indicated for diabetic neuropathy, the structure can be bioavailable and well-tolerated.<sup>[33]</sup> To determine the relevance of the thiocarbonyl rhodanine heterocycle itself, it was replaced with other heterocycles (R<sup>1</sup> and R<sup>2</sup>, Figure 6b) while the substituents R<sup>3</sup> and R<sup>4</sup> were

kept constant (corresponding to parts A and C in Figure 6a). In these experiments, rhodanines (R<sup>1</sup>=S and R<sup>2</sup>=S), thiohydantoin (R<sup>1</sup>=S and R<sup>2</sup>=N), thioxooxazolidinones (R<sup>1</sup>=S and R<sup>2</sup>=O), oxazolidinediones (R<sup>1</sup>=O and R<sup>2</sup>=O), and hydantoin (R<sup>1</sup>=O and R<sup>2</sup>=N) were synthesized and tested, and the following trend in the depolymerization of tau aggregates was observed: rhodanine (IC<sub>50</sub>/DC<sub>50</sub> (in  $\mu\text{M}$ ): 0.8/0.1) > thiohydantoin (6.1/0.4)  $\gg$  oxazolidinedione (3.5/2.2) = thioxooxazolidinone (3.1/2.4)  $\gg$  hydantoin (22.6/54.3). The IC<sub>50</sub> and DC<sub>50</sub> values represent, respectively, the assembly-inhibiting and disassembly-inducing half-maximal concentrations measured in vitro. The rhodanine heterocycle appeared to be the most potent, underlining the importance of the thioxo group in rhodanines, which is a known carboxylic acid bioisoster owing to its size, low electronegativity, and ability to engage in hydrogen bonds.<sup>[34]</sup> Also, the hydrophobicity of the sulfur atom may play an important role, as it leaves the amide part of the rhodanine heterocycle free for hydrogen bonding.

The substitution pattern on the heterocycle turned out to be crucial for activity. Hydrogen-bond acceptors in the form of nitro groups, carboxylic acids, phenols, or sulfonates/sulfonamides are often observed among amyloid aggregation inhibitors. The importance of the carboxylic acid (A, Figure 6a) and the impact of the substitution and tether connecting the central core to the carboxylic acid have been reported.<sup>[27]</sup> Esterification of the carboxylic acid or its replacement with an imidazole or benzimidazole group led to reduced disassembly activity in vitro (Table 1, compounds 1–4). Furthermore, the length of the linker between the carboxylic acid and the rhodanine core (B, Figure 6a) was investigated. These experiments revealed that increasing the distance to two C–C bonds resulted in an appreciable increase in the compound's inhibitory potency (Table 1, compounds 1, 5, and 6), thus indicating an optimal positioning of the inhibitor toward its binding site. Notably, these structural modifications aimed at optimizing the inhibitory potency did not concomitantly improve the disassembly activity. The biaryl part C of the compounds (Figure 6a) was varied to investigate the requirement of aromatic substitution. The heteroaromatic side chain (part C, Figure 6a) tolerated variations, but modifications on the furan heterocycle showed a trend for potency reduction (Table 1, compounds 1, 7–9), probably as a result of both electronic and steric factors. Replacement of the furan ring in 5 for thiophene in 7 (Table 1) slightly lowered the potency, as is also the case for the pyridine in 8 compared to the furan in 10.

In general, the presence of an aromatic side chain appeared necessary, supporting hydrophobic or  $\pi$  stacking interactions of this fragment.<sup>[36]</sup> Very bulky substituents, such as adamantyl or ferrocenyl, placed at the end of side chain C were generally well-tolerated, reducing only marginally the overall efficiency of the compounds. Introduction of a charged group by means of a carboxylic acid at the end of side chain C did not influence the potency considerably, underlining the structural adaptability around this position.<sup>[27]</sup> After optimization, an interesting 0.17  $\mu\text{M}$  IC<sub>50</sub> (compound 10, Table 1) could be obtained. The discrepancy between potencies observed in vitro and in the cell-based assay (see also

**Table 1:** Compound structures, IC<sub>50</sub> and DC<sub>50</sub> values, cytotoxicity, PHF inhibition in cell, and clogP values of rhodanine inhibitors.<sup>[a]</sup>

Compound	R <sup>3</sup>	R <sup>4</sup>	IC <sub>50</sub> <sup>[b]</sup> [μM]	DC <sub>50</sub> <sup>[b]</sup> [μM]	LDH <sup>[c]</sup> [%]	Inhibition in cells <sup>[d]</sup> [%]	clogP <sup>[e]</sup>
1			0.82	0.10	12.85 ± 20.82	20.40 ± 5.37	0.59
2			4.36	1.80	24.55 ± 3.83	N/D	4.35
3			0.67	0.94	6.14 ± 5.55	70.47 ± 4.49	5.30
4			1.09	0.80	5.91 ± 3.19	N/D	3.82
5			0.47	0.30	3.10 ± 7.80	21.55 ± 13.82	0.60
6			1.22	1.04	13.19 ± 9.55	N/D	0.65
7			0.97	0.77	N/D	N/D	1.07
8			5.03	1.66	7.58 ± 2.76	N/D	1.15
9			7.92	1.40	59.57 ± 4.52	N/D	1.26
10			0.17	0.13	16.49 ± 4.38	N/D	1.77

[a] The substituents R<sup>3</sup> and R<sup>4</sup> refer to the flanking regions on Figure 6 b; R<sup>1</sup> = R<sup>2</sup> = S. [b] The IC<sub>50</sub> and DC<sub>50</sub> values represent the assembly-inhibition and disassembly-inducing half-maximal concentrations measured in vitro by ThS assay. Each data point is the average of three experiments. The standard error of the mean of the IC<sub>50</sub> or DC<sub>50</sub> values determined from the curves was 10–20%. [c] The LDH (lactate dehydrogenase release) values describe the cytotoxicity of the compounds in N2a cells compared to the negative control set to 0% (dimethylsulfoxide, DMSO). Determined after incubation of the cells for 24 h with 10 μM compound. [d] The values obtained by incubating the cells with 15 μM compound correspond to the level of inhibition of tau aggregation normalized to a control without inhibitor (0%) in cells. N/D: not determined. [e] The calculated logarithms of water–octanol partition coefficients (clogP) were obtained using ChemDraw Ultra 10.0 software (CambridgeSoft).<sup>[35]</sup>

Figure 12 in Section 2.3) reflects the need for further optimization of this compound class with respect to ADME parameters (ADME = absorption distribution metabolism excretion) relevant for the in vivo activity. Whereas the toxicity was observed to be restricted to a safe range (2–8%, LDH assay in N2A cells, incubation 24 h with 10 μM compound, Figure 12), the negatively charged carboxylate group present on most compounds may limit their membrane permeability (clogP, Table 1). Among the obtained rhodanine derivatives, compound **3** is the most promising compound, as it achieved a 70 % reduction of aggregation in cells. The better efficiency on cells of this compound, which contains a charge-neutral benzimidazole group, may be attributed to improved permeability, a feature that would allow optimization of other inhibitors for in vivo potency by exchange of the carboxylate group for charge-neutral bioisosters.

Furthermore, the substances were also able to disaggregate preformed fibrils, a feature of prime importance. The mechanism behind this rare property is probably correlated to the trapping of the monomer or an assembly intermediate involved in the dynamic equilibrium between fibril and monomer, as also reported for Aβ aggregation.<sup>[37–39]</sup> Compounds may also be able to interact with the aggregated structure and disturb the protein–protein π-stacking arrangement of the fibrils. A different binding mode and different targets for inhibition and disaggregation on the complex aggregation pathway from the native nontoxic peptide to fibrils could therefore rationalize the loose correlation between observed IC<sub>50</sub> and DC<sub>50</sub> values.

There may be concerns about the toxicity of fragments generated by the disassembly of fibrils, because toxicity of small oligomers has been observed.<sup>[40,41]</sup> Nevertheless, studies



using compound **3** (Table 1) allowed us to observe the effect of tau filament disassembly on cellular viability. A clear reversal of the toxicity caused by tau aggregation in the cytosol was observed.<sup>[31]</sup> Also, recent reports on compounds binding to A $\beta$  fibrils indicate that many also bind to the oligomers and can have neuroprotective effects.<sup>[42]</sup>

## 2.2. Phenylthiazolylhydrazide Inhibitors

The application of in silico scaffold hopping to the data obtained from the original high-throughput screen of 200 000 compounds identified the phenylthiazolylhydrazide scaffold and two other leads that were not retrieved by the initial screen. The thiazolylhydrazide was selected for lead optimization and SAR investigation.<sup>[23]</sup> A collection of thiazolylhydrazides was obtained by synthetic derivatization of R<sup>1</sup>, R<sup>2</sup>, and R<sup>3</sup> (Figure 7b). The pharmacophore model obtained by

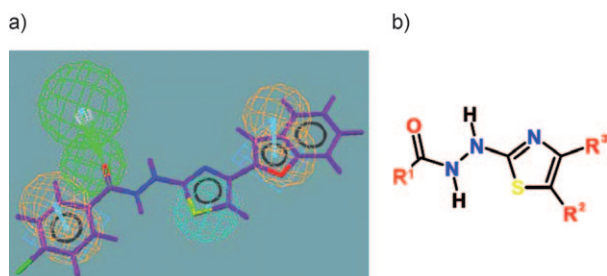


**Figure 7.** a) Four-feature pharmacophore model of thiazolylhydrazides. Aromatic rings (brown), hydrophobic region (blue), hydrogen-bond acceptor (green).<sup>[23]</sup> b) Core structure of the thiazolylhydrazides.

scaffold hopping stipulated two aromatic rings at R<sup>1</sup> and R<sup>3</sup>, a hydrophobic region on the thiazole ring, and a hydrogen-bond acceptor on the carboxyl amide (Figure 7a).

The virtual pharmacophore was confirmed and refined by experimental data obtained in tau aggregation and disaggregation assays, which are consistent with the SAR of the rhodanine-derived compounds. A structure superposition of the rhodanine core and the thiazolylhydrazine indicates obvious spatial similarities, which reflects common structural requirements for binding to a similar or identical site on tau aggregates or tau monomers (Figure 8).

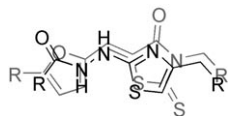


**Figure 8.** Superposition of the core structures of rhodanines and phenylthiazolylhydrazides, illustrating their close overlap.

An additional feature of the model that further improves the inhibitory potency is a hydrogen-binding substituent on R<sup>3</sup>, for example, the nitro group in BSc3094 (Figure 9). In parallel, the hydrophobic or  $\pi$ -stacking interactions on R<sup>1</sup> appeared to contribute to target

binding, as confirmed by saturation transfer difference (STD) NMR spectroscopy experiments, which revealed a strong interaction of the tau construct K18 with the R<sup>1</sup> aromatic ring (Figure 9). Moreover, the STD-NMR spectroscopy

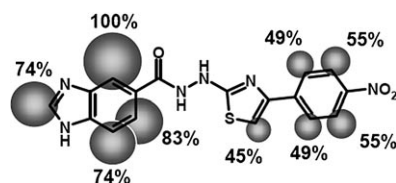


**Figure 9.** Binding epitope of inhibitor BSc3094 (class of phenylthiazolylhydrazides) with tau construct K18 derived from STD-NMR spectroscopy.<sup>[43]</sup> The percentages reflect the relative STD effects, which are representative of the binding affinities to the protein target.

copy experiments showed that the binding is specific, with a dissociation constant of 62  $\mu$ M.<sup>[43]</sup>

Although these compounds displayed lower in vitro potency than the rhodanines discussed above, their activity in cells appeared to be in the same range (see Figure 12 in Section 2.3), probably as a result of higher cell permeability. Nevertheless, these phenylthiazolylhydrazides also had a somewhat higher cytotoxicity (Figure 12).

## 2.3. N-Phenylamines and Anthraquinones

Further tau aggregation inhibitors were reported for the N-phenylamine and anthraquinone series.<sup>[25,30]</sup> These classes overlap only partially with the previously described SAR: the hydrogen-bonding substituents of the rhodanines and phenylthiazolylhydrazides are replaced by nitro groups or carboxylic acids on the N-phenylamines and by acidic aryl hydroxy groups on anthraquinones (Figures 10 and 11). The hydrophobic binding domains are provided by aromatic rings.

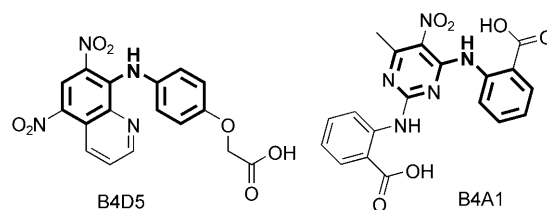


**Figure 10.** Structures of N-phenylamine-derived compounds.

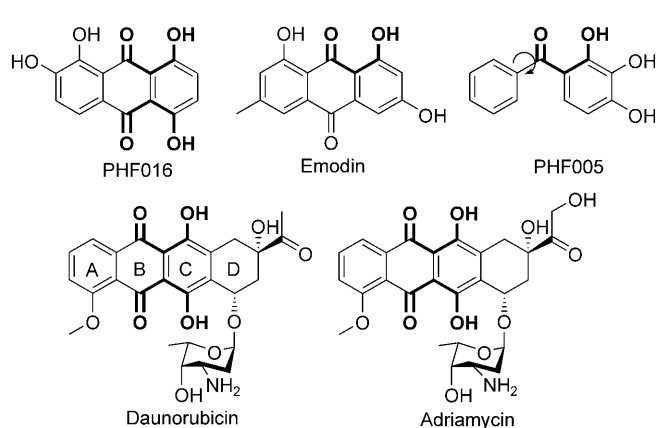


**Figure 11.** Structures of anthraquinone-derived compounds.

Compared with the two compound classes discussed above (rhodanines and phenylthiazolylhydrazides), the *N*-phenylamines displayed far lower potencies in vitro and in cells, together with 20% cytotoxicity (Figure 12), which hampers their use in vivo.

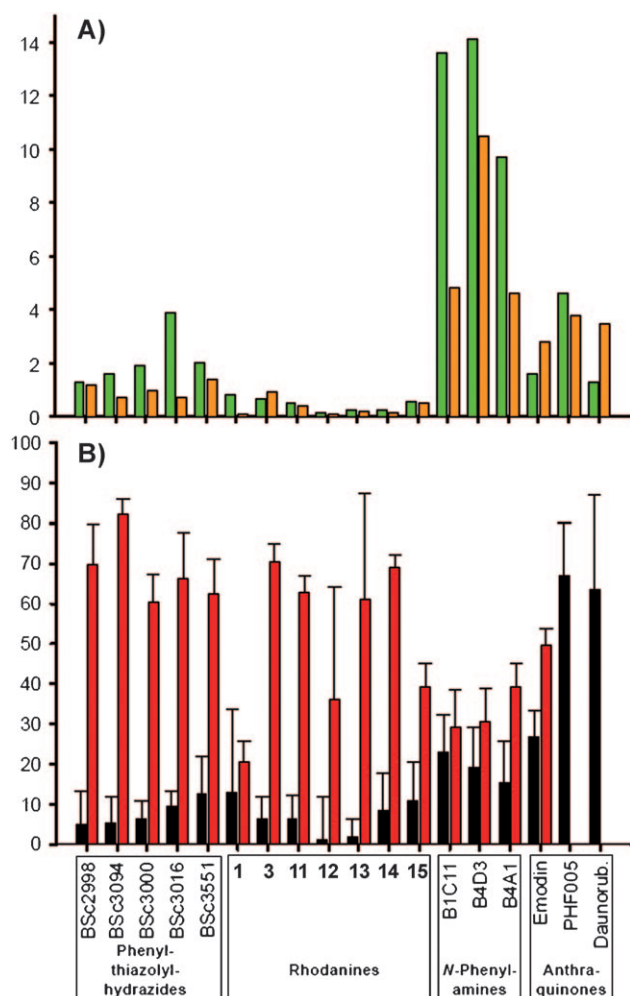


**Figure 12.** A) IC<sub>50</sub> values (green, in μM) for assembly inhibition and DC<sub>50</sub> values (orange, in μM) for disassembly induction and B) cytotoxicity (black, in %) and aggregation inhibitory activity in cells (red, in %). Cytotoxicity assay (LDH) was performed over 24 h in the presence of 10 μM compound. For testing the inhibitory activity in cells, the induced cells were treated with 15 μM compound over five days. The remaining aggregate-positive cells were quantified by ThS staining.<sup>[25, 27, 31, 43]</sup>

The anthraquinones all share a tricyclic structure with one or more β-hydroxyenone moieties (Figure 11). This last feature may play a significant role, as it is frequently observed in other inhibitor classes, such as flavonoids and naphthoquinones (see Sections 2.5 and 3). Catechins that do not have the keto functionality have a reduced potency.<sup>[44]</sup> Daunorubicin and adriamycin are further annelated and linked to a daunosamine sugar moiety (ring D, Figure 11). Notably, these two compounds are known as intercalating cytostatics and thus present a hazardous toxicological profile. Moreover, the cytotoxicity data (Figure 12) indicated substantial toxicity.

The five compounds depicted in Figure 11 were able to inhibit the aggregation of the K19 tau construct and also induced the disaggregation of preformed aggregates, with IC<sub>50</sub> values between 1.1 and 2.4 μM and DC<sub>50</sub> values between 2.2 and 3.8 μM.<sup>[25]</sup> One exception is compound PHF005, which showed a markedly lower activity, probably owing to its flexibility compared to closed tricyclic structures (rotation axis depicted by the arrow in Figure 11). Moreover, the substitutions on ring A (daunorubicin, Figure 11) did not appear to play a crucial role, as different patterns yielded similar inhibitory potencies. For ring D in daunorubicin and adriamycin to bear the sugar moiety does not give a competitive advantage compared to PHF016, thus indicating that the compounds are only moderately sensitive to the substitutions on that ring and accommodate even bulky substituents such as sugars. This finding could indicate a similar binding mode compared to rhodanines and phenylthiazolylhydrazides, for which bulky substituents were also tolerated on the far edges of the compound.

#### 2.4. Benzothiazoles

In addition to the above-mentioned data obtained from the screen of the 200 000 compound library,<sup>[22]</sup> several laboratories reported the identification of novel tau aggregation inhibitors, although the disassembly potencies of the compounds are rarely mentioned. Benzothiazole-based inhibitors have been described by Necula et al.,<sup>[45]</sup> and compound N744 is emphasized as an example (IC<sub>50</sub> = 300 nM, Figure 13).

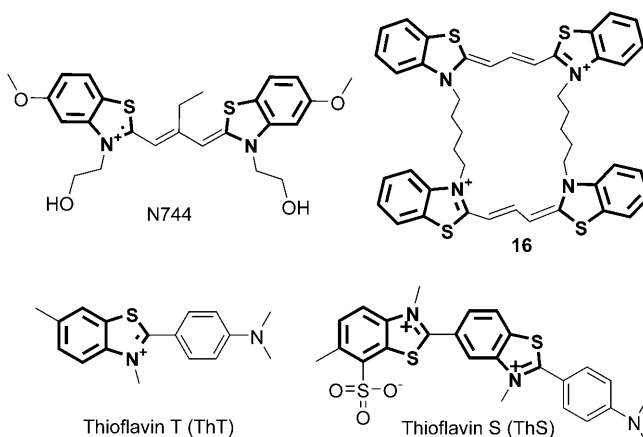


**Figure 13.** Structures of benzothiazole derivatives.

This thiocarbocyanine class presents a distinctive cationic charge that may interact with the target, probably mediated by charge–charge interactions, and contributes to the planarity of the structure. On the other edge, the benzothiazole heterocycle might provide hydrophobic interactions. This last feature probably accounts for the pronounced inhibitory activity in comparison with thioflavins like ThS or ThT, which are used as reporters of the β-sheet structure in the assembled state without affecting assembly as such.<sup>[45]</sup>

However, other reports document the loss of inhibitory activity of N744 at high concentration, caused by the



aggregation of the compound. This self-assembly process leads to *H*-aggregates that consist of columnar stacks of compound molecules with large slippage angles between successive molecular planes. By contrast, the N744 inhibitor has a monomeric or dimeric structure at low concentration that is considered to be the active form of the inhibitor.<sup>[46]</sup> A bivalent modification of N744 is able to simulate the dimeric structure by intramolecular interaction (compound **16**, Figure 13). Although compound **16** can form *H*-aggregates or a closed clamshell conformation, the four-fold improvement in activity was correlated to the open monomeric form, indicating that the improvement in potency results from the compound's multivalency and not from aggregation.<sup>[47]</sup>

## 2.5. Phenothiazines, Porphyrins, and Polyphenols

Taniguchi et al.<sup>[44]</sup> reported three classes of compounds active on tau aggregation inhibition on htau46 (htau34 isoform, 412 amino acids, first insert, four repeats) with  $IC_{50}$  values between 1.2  $\mu$ M (myrcetin, Figure 14) and 12  $\mu$ M

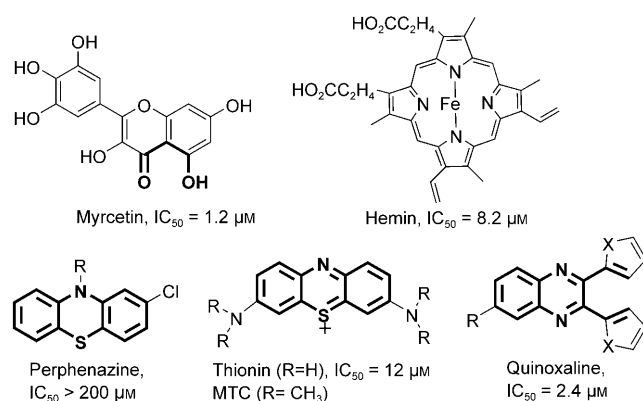


**Figure 14.** Tau aggregation inhibitors.<sup>[44]</sup>

(thionin). These classes included phenothiazines (thionin, perphenazine), porphyrins (hemin), and flavonoid polyphenols (myrcetin). The phenols share the SAR described above for the anthraquinones with the characteristic  $\beta$ -hydroxyenone pattern (myrcetin, Figure 14), which is also present on the naphthoquinone rifamycin as a tautomer.<sup>[44]</sup>

The phenothiazines are tricyclic structures (thionin, Figure 14) that incorporate sulfur and nitrogen atoms on the central heterocycle. They are similar to the above-mentioned benzothiazole inhibitors, sharing positively charged atoms and hydrophobic aromatic groups. The charge-neutral phenothiazines are reported to have good blood–brain barrier permeability, as confirmed by their use as antipsychotic drugs. The planarity and aromaticity of the central heterocycle appears to be the determining factor for inhibition of tau aggregation, since nonconjugated nonplanar analogues such as perphenazine display dramatically reduced potency (Figure 14). The positive charge on thionin or MTC most likely plays a secondary role, since charge-neutral quinoxalines, which overlap strongly with the phenothiazines (Figure 14), were also reported as potent tau aggregation

inhibitors.<sup>[48]</sup> The methylthioninium chloride compound (MTC, also known as methylene blue) was recently reported as a potent in vivo tau aggregation inhibitor with submicromolar  $IC_{50}$  values in cells.<sup>[49,50]</sup> Moreover, the results of a phase II clinical trial indicated a significantly lower rate of decline of cognitive functions compared to placebo. MTC was orally administered in a double-blind, randomized parallel-design phase-II trial to 321 participants over 84 weeks. The reported results at 50 weeks for patients with mild to moderate cognitive impairment showed an ADAS-cog score decline of seven points for placebo versus one point for the MTC cohort, equivalent to an 81 % reduction of the cognitive decline rate under MTC ( $p < 0.0001$ ). The results were supported by SPECT and PET brain imaging. Although data on pharmacodynamics and pharmacokinetics are currently not published, the confirmation of these data would represent a breakthrough for the management of Alzheimer's disease and a proof of concept for the tau aggregation inhibition strategy.

The porphyrins (hemin, Figure 14) are the only organo-metallic examples of tau aggregation inhibitors and probably bind differently than the other reported inhibitors. The inhibitory activity is dependent on a central metal (iron or zinc), and the phthalocyanine compound lacking the metal center is a weaker inhibitor by one to two orders of magnitude.<sup>[44,51]</sup> Howlett et al. reported the inhibitory potency of porphyrins on A $\beta$ 42 amyloid aggregation<sup>[51]</sup> and hypothesized that the iron center might coordinate histidine residues on the target, a mechanism that might be transposed to tau aggregation inhibition as well.

Similarities in the amyloid ultrastructure support a partially shared binding mode for their inhibitors. Indeed, amyloid fibrils, irrespective of their amino acid sequence, share a common X-ray diffraction pattern showing a characteristic 4.6–4.8 Å meridional reflection. This value corresponds to the spacing between the peptide chains forming a cross- $\beta$ -sheet structure such that the  $\beta$  strands of the proteins are arranged perpendicular to the fibril axis. Furthermore, AFM analysis of A $\beta$ 42 aggregates in reconstituted membranes revealed a remarkable supramolecular ion-channel-like structure,<sup>[52,53]</sup> a striking feature of most amyloids, such as  $\alpha$ -synuclein, A $\beta$ 42, IAPP, and others. Irrespective of their amino acid sequence, some of the soluble oligomeric amyloids also share a common structure that is recognized by specific antibodies that neutralize their toxicity.<sup>[54]</sup> The same conformational antibody recognized oligomers formed by IAPP,  $\alpha$ -synuclein, A $\beta$ 42, polyglutamine, and other proteins. This shared recognition by the antibody implies a structural link between these oligomers that fibrillar aggregates might subsequently inherit.<sup>[55,56]</sup> These similarities correlate with the observation that aggregation inhibitors of a particular amyloid class are potential inhibitors of a wide variety of other amyloids<sup>[44,57–59]</sup> and that histological stains such as ThS or Congo red bind to aggregates in at least fifteen genetically unrelated disorders.<sup>[60]</sup>

The detailed investigation of A $\beta$  aggregation is therefore an important asset for the understanding of amyloidosis in a broader sense. Strategies for the prevention of A $\beta$  misfolding and aggregation are well documented in the literature.<sup>[61–63]</sup>

### 3. Aggregation Inhibitors for Other Amyloidogenic Proteins

Investigation of pathways to A $\beta$ 42 fibrillization indicated that the equilibrium between the assembly forms might be influenced by small molecules.<sup>[40]</sup> Using an oligomer-specific antibody as a primary read-out, it was possible to analyze the influence of reported amyloid aggregation inhibitors. The compounds were classified in three categories: 1) inhibitors of oligomerization but not fibrillization, 2) inhibitors of both oligomerization and fibrillization, and 3) inhibitors of fibrillization but not oligomerization. Notably, the oligomerization inhibitors (first category) appeared also to be promoters of fibrillization. The full inhibitors (second category) include meclocycline sulfosalicylate, hemin, and *ortho*-vanillin (with IC<sub>50</sub> < 10  $\mu$ M), belonging to the anthraquinone, porphyrin, and polyphenol compound classes, respectively, which are also described above as tau aggregation inhibitors.

The potency differences between amyloid aggregation inhibitors could correlate with the affinity of the compounds for the side-chain residues on the fibrils. Inhibitors of tau aggregation are less common than  $\beta$ -amyloid inhibitors, as illustrated by the comparative inhibition potencies of eight compound classes by Taniguchi et al.<sup>[44]</sup> This scarcity might be due in part to the lack of aromatic residues on tau compared to A $\beta$ , which limits the potential for hydrophobic interactions with the inhibitors. An example of a different SAR between tau and A $\beta$ 40 inhibitors is revealed by the comparison of anthracycline potencies: whereas tau aggregation is insensitive to the substituents on ring D (see Figure 11), only anthracyclines bearing the daunosamine sugar substituent (e.g. doxorubicin) appeared active on A $\beta$ 40.<sup>[64]</sup> A pharmacophore mapping of the anthracyclines as A $\beta$  aggregation inhibitors yielded a three-point model with the aromatic rings serving as hydrophobic regions and the sugar moiety as hydrogen-bond donor and acceptor (Figure 15).

Polyphenols, for example myricetin (Figure 14), are presented above (Section 2.5) as tau aggregation inhibitors. These compounds show inhibitory activity on a variety of amyloids, such as  $\alpha$ -synuclein, IAPP, A $\beta$ 40, PrP<sup>Sc</sup>, and tau.<sup>[58]</sup> Polyphenols are characterized by the presence of several phenol functionalities (Figure 16). These substances are often observed in higher plants, such as ginkgo biloba, tea bush, grape, or turmeric. Polyphenols are categorized according to their structure in flavonoids, tannic acids, and lignins (Figure 16). Although a discussion persists on whether their

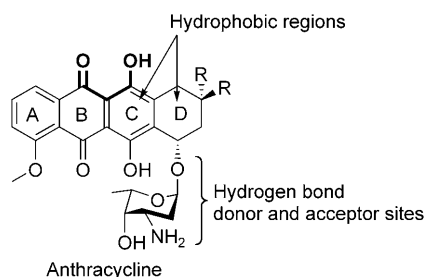


**Figure 15.** SAR for anthracyclines on the inhibition of A $\beta$ 40 aggregation.

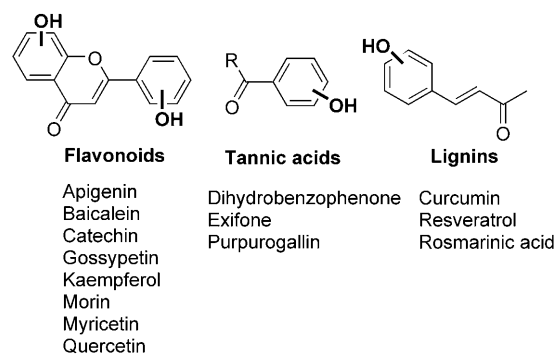


**Figure 16.** Polyphenol inhibitors.

in vivo activity is linked to their antioxidant properties, the in vitro data clearly indicate that they interfere with the elongation phase of fibril assembly.<sup>[64,65]</sup> However, they commonly display a very high metabolic turnover, which is frequently manifested in reduced oral bioavailability and reduced penetration of the blood–brain barrier, thus significantly minimizing their potential as lead structures.

A common requirement for aggregation inhibitor activity between tau and A $\beta$  is the presence of hydroxy groups on the phenolic moiety (Figure 16), as ether analogues display a reduced inhibitory activity. Phenolic hydroxy groups are known for their greater acidity than aliphatic hydroxy groups and for their ability to form hydrogen bonds. The crucial role of hydrogen bonding or hydrophilicity was also observed for the scyllo-inositol inhibitor.<sup>[66]</sup> Furthermore, some of the lignins (e.g. curcumin) are symmetrical, and an optimal length of 16–19 Å between the phenolic rings is reported to be most favorable for A $\beta$ 40 (Figure 17).<sup>[67]</sup>

Curcumin was identified in cellular assays to interfere with several processes linked to neurodegenerative diseases. Nevertheless, the poor oral absorption and blood–brain barrier permeability of curcumin in mammals considerably limits its potential application in vivo. The replacement of the  $\beta$ -hydroxyenone functionality in curcumin with substituted pyrazoles yielded inhibitors of A $\beta$  and tau aggregation.<sup>[68]</sup> The interaction with A $\beta$  required linear pyrazoles, which enhanced the selectivity of the interference of Y-shaped derivatives with tau aggregates. Thus, the activities diverged in branched derivatives featuring *N*-aryl substituents. The most active 4-nitrophenyl- and 3-nitrophenyl-substituted curcumin pyrazoles displayed tau aggregation inhibition at low micromolar concentrations. The introduction of an electron-withdrawing group on the *N*-aryl pyrazoles increased the inhibition of tau aggregation 100-fold relative to the parent *N*-phenylpyrazole. A similar SAR was observed for disaggregation of tau protein. The introduction of a nitro group on the *N*-aryl pyrazoles increased the tau depolymer-

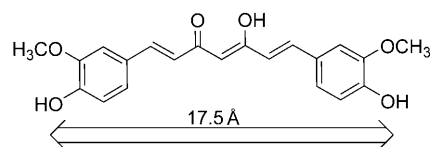


**Figure 17.** Structure of curcumin (enol form).

ization activity 18–70-fold relative to the parent *N*-phenylpyrazole.<sup>[68]</sup>

#### 4. Binding Mode

The complex folding pathways from nontoxic native monomeric peptides to fibrils imply the simultaneous presence of various potential targets for aggregation inhibitors and disaggregators.<sup>[2,69]</sup> Investigation of the structure of the early aggregation intermediates and their small-molecule binding partners is still in its infancy. The binding epitopes obtained by STD-NMR spectroscopy for interaction between a phenylthiazolylhydrazide inhibitor and a monomeric tau peptide (see Figure 9 in Section 2.2) illustrate that this type of interaction may be a common feature among aggregation inhibitors and disaggregation promoters.

The binding mode to mature fibrils appears to involve hydrophobic interactions and hydrogen bonding. A binding model for Congo red on A $\beta$  has been derived from the X-ray structure of Congo red binding to the  $\beta$  sheets of insulin dimers.<sup>[70]</sup> Although Congo red and ThS or ThT are reported to be only weak inhibitors of aggregation,<sup>[46]</sup> competition studies indicate that their binding site accommodates ligands from other chemical classes<sup>[71]</sup> and hence could overlap with reported inhibitors, such as N744.<sup>[45]</sup> Moreover, the competitive binding of the tau aggregation inhibitor N744 with common  $\beta$ -amyloid binders such as ThS might suggest similar binding modes of thioflavins and Congo red on tau and  $\beta$ -amyloid fibrils. The aromatic interactions play a predominant role in this model, in which the inhibitor is intercalated parallel to the peptide chain (Figure 18, model A).

A perpendicular orientation has also been proposed,<sup>[72,73]</sup> consistent with charge–charge interactions between positively charged residues on the fibril and the negatively charged sulfonic acids of Congo red. The binding was proposed to span perpendicularly across five peptide chains, on the basis of the distance between the sulfonic acid functionalities (19 Å, Figure 18, model B). This optimal distance also fits well with the reported optimized size observed for curcumin analogues. Support for this transverse binding mode came from linear birefringence imaging of Congo red stained amyloid plaques, which illustrate binding perpendicular to the

peptide arrangement (similar to model B, Figure 18).<sup>[59]</sup> It is noteworthy that a similar binding mode for thioflavin T on bovine insulin and  $\beta$ -lactoglobulin has been obtained by confocal microscopy with polarized laser light.<sup>[74]</sup> Such models are consistent with the change in fluorescence spectra and intensity observed upon binding of stains to fibrils, since the reduced flexibility of the entrapped molecule into the fibril groove (model B) is expected to enhance the fluorescence quantum yield of the compound.<sup>[74]</sup>

A third model has been proposed on the basis of the pH-dependent binding of Congo red to A $\beta$ 40 amyloid peptides, suggesting at physiological pH values an electrostatic interaction between positively charged histidine residues on the protein and anionic sulfonate groups on the Congo red molecule.<sup>[75]</sup> The model suggests a regular alignment of histidine residues pointing out of the periphery of a  $\beta$ -helix nanotube or a parallel  $\beta$ -sheet protofilament, forming a template for the assembly of Congo red (model C, Figure 18). The resulting interactions would promote the self-assembly of Congo red, resulting in the bathochromic shift in UV/vis absorption characteristic of *J*-aggregates. The self-assembly of carbocyanines and porphyrins to form *H*- or *J*-aggregates is well-documented, with attractive interactions between the  $\pi$  systems as the driving force. The cryo-TEM micrographs of such aggregates revealed a striking supramolecular superhelix structure (Figure 19).<sup>[76]</sup>

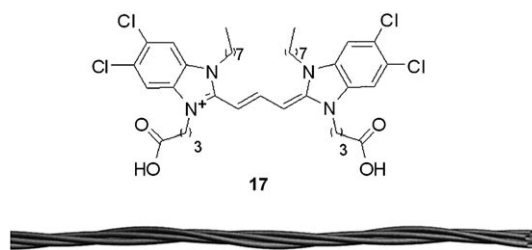


**Figure 19.** Cryo-TEM micrograph reconstitution of *J*-aggregates formed by carbocyanine 17.<sup>[76]</sup>

#### 5. Summary and Outlook

The identification of aggregation inhibitors and the investigation of their binding mode is an important step toward addressing fundamental issues of amyloid formation and its pathological consequences. Moreover, it is intriguing that even extracellular A $\beta$  oligomers or aggregates, commonly considered the major culprits of Alzheimer's disease, exert their toxic function through tau as a constitutive intracellular component.<sup>[77–81]</sup> The understanding of the complex self-assembly processes involved in fibril formation and its inhibition mechanism by small molecules requires multidisciplinary efforts. Common structural features between different compound classes are starting to emerge, with the presence of aromatic/hydrophobic patches and hydrogen-bonding elements along flat extended structures.

In the case of tau, the current in vitro nanomolar IC<sub>50</sub> values for N744, rhodanines, and phenylthiazolylhydrazide encourage the search for improved potencies in aggregation

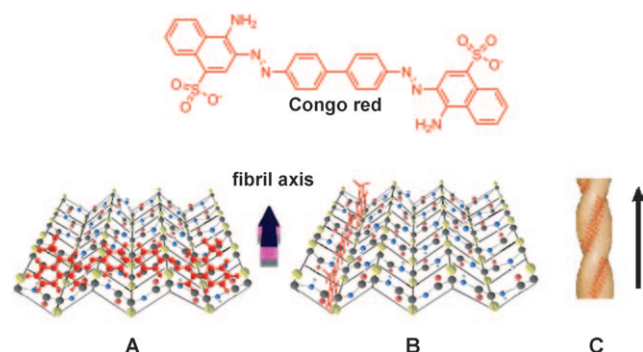


**Figure 18.** Structure of Congo red and binding model to amyloids. A) Binding parallel to the  $\beta$  sheets. B) Binding perpendicular to the  $\beta$  sheets. C) Aggregation of Congo red (red lines) on the helical fibril structure.



inhibition, with particular emphasis on disaggregation ability, permeability, and cytotoxicity. The design of cell-permeable compounds is a key step in the future development of new generations of aggregation inhibitors. Especially the negative or positive charges shared by most aggregation inhibitors impede membrane permeability. The successful compound optimization toward charge-neutral, cell-permeable structures is illustrated by the design of imaging agents for diagnosis such as Pittsburgh compound B (PIB) or methoxy-X04, inspired by the poorly permeable thioflavins and Congo red analogues, respectively.<sup>[73,82–86]</sup> Preliminary investigations using a charge-neutral compound of moderate in vitro activity such as **3** (Table 1) allowed the study of the effects of tau filament disassembly on cellular viability, which resulted in the prevention or reversal of the toxicity caused by tau aggregation in the cytosol.<sup>[31]</sup> This observation highlights the role of tau as a key player in neurodegenerative processes.<sup>[87,88]</sup>

A striking property shared by many aggregation inhibitors is their ability to form *H*- or *J*-aggregates. Better than promiscuous nonspecific inhibitors resulting from unordered micelles,<sup>[89,90]</sup> these self-assembly properties might indicate the opportunity to optimize amyloid inhibitors through supramolecular structures with improved specificity and potency, although the drug formulation and ADME optimization might turn out to be challenging.<sup>[76,91–93]</sup>

Also, in the current discussion on neuronal toxicity mediated by small oligomers,<sup>[40,41]</sup> it has been recently suggested that interventions that reduce amyloid load but increase small oligomers could be harmful.<sup>[94]</sup> In principle, it is therefore necessary to determine the binding properties of the inhibitor compounds to the small oligomeric amyloid precursors. The recent finding that ThT and Congo red bind to A $\beta$  oligomers and have neuroprotective effects are encouraging and underscore the potential of the compounds as therapeutics for amyloid-related pathologies.<sup>[42]</sup>

*Financial support was received from the Institute for the Study on Aging (New York), the Deutsche Forschungs-Gemeinschaft, the European Union ("Europäischer Fond für regionale Entwicklung" and Memosad Project of 7th FP), the Volkswagen Foundation, and the State of North Rhine-Westphalia. We thank Gregor Larbig (Darmstadt), Atilla Coksezen (Hamburg), and Inna Khlistunova (Hamburg) for performing some of the experiments, and Bernd Meyer (Hamburg) for stimulating discussions.*

Received: June 4, 2008

Revised: August 6, 2008

Published online: February 2, 2009

- [1] J. W. Kelly, *Nat. Struct. Biol.* **2002**, 9, 323.
- [2] H. LeVine, *Curr. Med. Chem.* **2002**, 9, 1121.
- [3] M. Townsend, J. P. Cleary, T. Mehta, J. Hofmeister, S. Lesne, E. O'Hare, D. M. Walsh, D. J. Selkoe, *Ann. Neurol.* **2006**, 60, 668.
- [4] L. Lecanu, W. Yao, G. L. Teper, Z. X. Yao, J. Greeson, V. Papadopoulos, *Steroids* **2004**, 69, 1.
- [5] L. Jenagaratnam, R. McShane, *Cochrane Database Syst. Rev.* **2006**, CD005380.

- [6] E. Sampson, L. Jenagaratnam, R. McShane, *Cochrane Database Syst. Rev.* **2008**, CD005380.
- [7] M. R. Sawaya, S. Sambashivan, R. Nelson, M. I. Ivanova, S. A. Sievers, M. I. Apostol, M. J. Thompson, M. Balbirnie, J. J. Wiltzius, H. T. McFarlane, A. O. Madsen, C. Riekel, D. Eisenberg, *Nature* **2007**, 447, 453.
- [8] M. N. Vieira, L. Forny-Germano, L. M. Saraiva, A. Sebollela, A. M. Martinez, J. C. Houzel, F. G. De Felice, S. T. Ferreira, *J. Neurochem.* **2007**, 103, 736.
- [9] K. Leroy, A. Bretteville, K. Schindowski, E. Gilissen, M. Authet, R. De Decker, Z. Yilmaz, L. Buee, J. P. Brion, *Am. J. Pathol.* **2007**, 171, 976.
- [10] C. Ballatore, V. M. Lee, J. Q. Trojanowski, *Nat. Rev. Neurosci.* **2007**, 8, 663.
- [11] M. Kidd, *Nature* **1963**, 197, 192.
- [12] P. Friedhoff, M. von Bergen, E. M. Mandelkow, E. Mandelkow, *Biochim. Biophys. Acta Mol. Basis Dis.* **2000**, 1502, 122.
- [13] H. Inouye, D. Sharma, W. J. Goux, D. A. Kirschner, *Biophys. J.* **2005**, 90, 1774.
- [14] K. Arima, *Neuropathology* **2006**, 26, 475.
- [15] R. Guerrero, P. Navarro, E. Gallego, J. Avila, J. G. de Yébenes, M. P. Sanchez, *J. Alzheimer's Dis.* **2008**, 13, 161.
- [16] C. Haass, D. J. Selkoe, *Nat. Rev. Mol. Cell Biol.* **2007**, 8, 101.
- [17] M. von Bergen, P. Friedhoff, J. Biernat, J. Heberle, E. M. Mandelkow, E. Mandelkow, *Proc. Natl. Acad. Sci. USA* **2000**, 97, 5129.
- [18] M. D. Mukrasch, P. Markwick, J. Biernat, M. Bergen, P. Bernado, C. Griesinger, E. Mandelkow, M. Zweckstetter, M. Blackledge, *J. Am. Chem. Soc.* **2007**, 129, 5235.
- [19] M. D. Mukrasch, M. von Bergen, J. Biernat, D. Fischer, C. Griesinger, E. Mandelkow, M. Zweckstetter, *J. Biol. Chem.* **2007**, 282, 12230.
- [20] I. Kelleher, C. Garwood, D. P. Hanger, B. H. Anderton, W. Noble, *J. Neurochem.* **2007**, 103, 2256.
- [21] K. S. Kosik, H. Shimura, *Biochim. Biophys. Acta Mol. Basis Dis.* **2005**, 1739, 298.
- [22] M. Pickhardt, M. von Bergen, Z. Gazova, A. Hascher, J. Biernat, E. M. Mandelkow, E. Mandelkow, *Curr. Alzheimer Res.* **2005**, 2, 219.
- [23] G. Larbig, M. Pickhardt, D. G. Lloyd, B. Schmidt, E. Mandelkow, *Curr. Alzheimer Res.* **2007**, 4, 315.
- [24] P. Friedhoff, A. Schneider, E. M. Mandelkow, E. Mandelkow, *Biochemistry* **1998**, 37, 10223.
- [25] M. Pickhardt, Z. Gazova, M. von Bergen, I. Khlistunova, Y. Wang, A. Hascher, E. M. Mandelkow, J. Biernat, E. Mandelkow, *J. Biol. Chem.* **2005**, 280, 3628.
- [26] J. H. Zhang, T. D. Chung, K. R. Oldenburg, *J. Biomol. Screening* **1999**, 4, 67.
- [27] B. Bulic, M. Pickhardt, I. Khlistunova, J. Biernat, E. M. Mandelkow, E. Mandelkow, H. Waldmann, *Angew. Chem.* **2007**, 119, 9375; *Angew. Chem. Int. Ed.* **2007**, 46, 9215.
- [28] A. Schneider, J. Biernat, M. von Bergen, E. Mandelkow, E. M. Mandelkow, *Biochemistry* **1999**, 38, 3549.
- [29] S. Barghorn, P. Davies, E. Mandelkow, *Biochemistry* **2004**, 43, 1694.
- [30] M. Pickhardt, J. Biernat, I. Khlistunova, Y. P. Wang, Z. Gazova, E. M. Mandelkow, E. Mandelkow, *Curr. Alzheimer Res.* **2007**, 4, 397.
- [31] I. Khlistunova, M. Pickhardt, J. Biernat, Y. Wang, E. M. Mandelkow, E. Mandelkow, *Curr. Alzheimer Res.* **2007**, 4, 544.
- [32] E. E. Carlson, J. F. May, L. L. Kiessling, *Chem. Biol.* **2006**, 13, 825.
- [33] N. Hotta, Y. Akanuma, R. Kawamori, K. Matsuoka, Y. Oka, M. Shichiri, T. Toyota, M. Nakashima, I. Yoshimura, N. Sakamoto, Y. Shigeta, *Diabetes Care* **2006**, 29, 1538.
- [34] G. A. Patani, E. J. LaVoie, *Chem. Rev.* **1996**, 96, 3147.
- [35] A. J. Leo, *Chem. Rev.* **1993**, 93, 1281.

- [36] M. L. Waters, *Curr. Opin. Chem. Biol.* **2002**, *6*, 736.
- [37] M. von Bergen, S. Barghorn, J. Biernat, E. M. Mandelkow, E. Mandelkow, *Biochim. Biophys. Acta Mol. Basis Dis.* **2005**, *1739*, 158.
- [38] J. D. Harper, P. T. Lansbury, Jr., *Annu. Rev. Biochem.* **1997**, *66*, 385.
- [39] Y. Matsuoka, M. Saito, J. LaFrancois, K. Gaynor, V. Olm, L. Wang, E. Casey, Y. Lu, C. Shiratori, C. Lemere, K. Duff, *J. Neurosci.* **2003**, *23*, 29.
- [40] M. Necula, R. Kaye, S. Milton, C. G. Glabe, *J. Biol. Chem.* **2007**, *282*, 10311.
- [41] H. A. Lashuel, D. Grillo-Bosch, *Methods Mol. Biol.* **2005**, *299*, 19.
- [42] I. Maezawa, H. S. Hong, R. Liu, C. Y. Wu, R. H. Cheng, M. P. Kung, H. F. Kung, K. S. Lam, S. Oddo, F. M. Laferla, L. W. Jin, *J. Neurochem.* **2008**, *104*, 457.
- [43] M. Pickhardt, G. Larbig, I. Khlistunova, A. Coksezen, B. Meyer, E. M. Mandelkow, B. Schmidt, E. Mandelkow, *Biochemistry* **2007**, *46*, 10016.
- [44] S. Taniguchi, N. Suzuki, M. Masuda, S. Hisanaga, T. Iwatsubo, M. Goedert, M. Hasegawa, *J. Biol. Chem.* **2005**, *280*, 7614.
- [45] M. Necula, C. N. Chirita, J. Kuret, *Biochemistry* **2005**, *44*, 10227.
- [46] E. E. Congdon, M. Necula, R. D. Blackstone, J. Kuret, *Arch. Biochem. Biophys.* **2007**, *465*, 127.
- [47] N. S. Honson, J. R. Jensen, M. V. Darby, J. Kuret, *Biochem. Biophys. Res. Commun.* **2007**, *363*, 229.
- [48] A. Crowe, C. Ballatore, E. Hyde, J. Q. Trojanowski, V. M. Lee, *Biochem. Biophys. Res. Commun.* **2007**, *358*, 1.
- [49] "Preparation of phenothiazine derivatives for treatment of tauopathy": C. M. Wischik, J. E. Rickard, C. R. Harrington, D. Horsley, J. M. D. Storey, C. Marshall, J. P. Sinclair, PCT Int. Appl. WO 2007110630, **2007**.
- [50] C. M. Wischik, P. C. Edwards, R. Y. Lai, M. Roth, C. R. Harrington, *Proc. Natl. Acad. Sci. USA* **1996**, *93*, 11213.
- [51] D. Howlett, P. Cutler, S. Heales, P. Camilleri, *FEBS Lett.* **1997**, *417*, 249.
- [52] A. Quist, I. Doudevski, H. Lin, R. Azimova, D. Ng, B. Frangione, B. Kagan, J. Ghiso, R. Lal, *Proc. Natl. Acad. Sci. USA* **2005**, *102*, 10427.
- [53] H. A. Lashuel, P. T. Lansbury, Jr., *Q. Rev. Biophys.* **2006**, *39*, 167.
- [54] R. Kaye, E. Head, J. L. Thompson, T. M. McIntire, S. C. Milton, C. W. Cotman, C. G. Glabe, *Science* **2003**, *300*, 486.
- [55] R. Kaye, E. Head, F. Sarsoza, T. Saing, C. W. Cotman, M. Necula, L. Margol, J. Wu, L. Breydo, J. L. Thompson, S. Rasool, T. Gurlo, P. Butler, C. G. Glabe, *Mol. Neurodegener.* **2007**, *2*, 18.
- [56] C. G. Glabe, *Trends Biochem. Sci.* **2004**, *29*, 542.
- [57] V. Heiser, S. Engemann, W. Brocker, I. Dunkel, A. Boeddrich, S. Waelter, E. Nordhoff, R. Lurz, N. Schugardt, S. Rautenberg, C. Herhaus, G. Barnickel, H. Bottcher, H. Lehrach, E. E. Wanker, *Proc. Natl. Acad. Sci. USA* **2002**, *99*, 16400.
- [58] Y. Porat, A. Abramowitz, E. Gazit, *Chem. Biol. Drug Des.* **2006**, *67*, 27.
- [59] L. W. Jin, K. A. Claborn, M. Kurimoto, M. A. Geday, I. Maezawa, F. Sohraby, M. Estrada, W. Kaminsky, B. Kahr, *Proc. Natl. Acad. Sci. USA* **2003**, *100*, 15294.
- [60] J. W. Kelly, *Curr. Opin. Struct. Biol.* **1996**, *6*, 11.
- [61] L. D. Estrada, C. Soto, *Curr. Top. Med. Chem.* **2007**, *7*, 115.
- [62] C. Soto, L. Estrada, *Subcell. Biochem.* **2005**, *38*, 351.
- [63] S. Bieler, C. Soto, *Curr. Drug Targets* **2004**, *5*, 553.
- [64] D. R. Howlett, A. R. George, D. E. Owen, R. V. Ward, R. E. Markwell, *Biochem. J.* **1999**, *343*, 419.
- [65] F. Yang, G. P. Lim, A. N. Begum, O. J. Ubeda, M. R. Simmons, S. S. Ambegaokar, P. P. Chen, R. Kaye, C. G. Glabe, S. A. Frautschy, G. M. Cole, *J. Biol. Chem.* **2005**, *280*, 5892.
- [66] J. McLaurin, R. Golomb, A. Jurewicz, J. P. Antel, P. E. Fraser, *J. Biol. Chem.* **2000**, *275*, 18495.
- [67] A. A. Reinke, J. E. Gestwicki, *Chem. Biol. Drug Des.* **2007**, *70*, 206.
- [68] R. Narlawar, M. Pickhardt, S. Leuchtenberger, K. Baumann, S. Krause, T. Dyrks, S. Weggen, E. Mandelkow, B. Schmidt, *ChemMedChem* **2008**, *3*, 165.
- [69] D. R. Howlett, *Curr. Med. Chem. Immunol. Endocr. Metab. Agents* **2001**, *1*, 25.
- [70] D. B. Carter, K. C. Chou, *Neurobiol. Aging* **1998**, *19*, 37.
- [71] L. Ye, J. L. Morgenstern, A. D. Gee, G. Hong, J. Brown, A. Lockhart, *J. Biol. Chem.* **2005**, *280*, 23599.
- [72] W. E. Klunk, M. L. Debnath, J. W. Pettegrew, *Neurobiol. Aging* **1994**, *15*, 691.
- [73] W. E. Klunk, J. W. Pettegrew, D. J. Abraham, *J. Histochem. Cytochem.* **1989**, *37*, 1273.
- [74] M. R. Krebs, E. H. Bromley, A. M. Donald, *J. Struct. Biol.* **2005**, *149*, 30.
- [75] H. Inouye, D. A. Kirschner, *Subcell. Biochem.* **2005**, *38*, 203.
- [76] H. Von Berlepsch, C. Böttcher, A. Ouart, C. Burger, S. Dähne, S. Kirstein, *J. Phys. Chem. B* **2000**, *104*, 5255.
- [77] P. Talaga, L. Quere, *Curr. Drug Targets CNS Neurol. Disord.* **2002**, *1*, 567.
- [78] S. Y. Park, A. Ferreira, *J. Neurosci.* **2005**, *25*, 5365.
- [79] E. D. Roberson, K. Searce-Levie, J. J. Palop, F. Yan, I. H. Cheng, T. Wu, H. Gerstein, G. Q. Yu, L. Mucke, *Science* **2007**, *316*, 750.
- [80] M. E. King, H. M. Kan, P. W. Baas, A. Erisir, C. G. Glabe, G. S. Bloom, *J. Cell Biol.* **2006**, *175*, 541.
- [81] M. Rapoport, H. N. Dawson, L. I. Binder, M. P. Vitek, A. Ferreira, *Proc. Natl. Acad. Sci. USA* **2002**, *99*, 6364.
- [82] B. P. Kinosian, E. Stallard, J. H. Lee, M. A. Woodbury, A. S. Zbrozek, H. A. Glick, *J. Am. Geriatr. Soc.* **2000**, *48*, 631.
- [83] W. E. Klunk, B. J. Lopresti, M. D. Ikonovic, I. M. Lefterov, R. P. Koldamova, E. E. Abrahamson, M. L. Debnath, D. P. Holt, G. F. Huang, L. Shao, S. T. DeKosky, J. C. Price, C. A. Mathis, *J. Neurosci.* **2005**, *25*, 10598.
- [84] C. A. Mathis, B. J. Lopresti, W. E. Klunk, *Nucl. Med. Biol.* **2007**, *34*, 809.
- [85] W. E. Klunk, B. J. Bacskai, C. A. Mathis, S. T. Kajdasz, M. E. McLellan, M. P. Frosch, M. L. Debnath, D. P. Holt, Y. Wang, B. T. Hyman, *J. Neuropathol. Exp. Neurol.* **2002**, *61*, 797.
- [86] L. Cai, R. B. Innis, V. W. Pike, *Curr. Med. Chem.* **2007**, *14*, 19.
- [87] M. Meyer-Luehmann, T. L. Spires-Jones, C. Prada, M. Garcia-Alloza, A. de Calignon, A. Rozkalne, J. Koenigsnecht-Talboo, D. M. Holtzman, B. J. Bacskai, B. T. Hyman, *Nature* **2008**, *451*, 720.
- [88] K. F. Winklhofer, J. Tatzelt, C. Haass, *EMBO J.* **2008**, *27*, 336.
- [89] S. L. McGovern, B. T. Helfand, B. Feng, B. K. Shoichet, *J. Med. Chem.* **2003**, *46*, 4265.
- [90] B. Y. Feng, B. H. Toyama, H. Wille, D. W. Colby, S. R. Collins, B. C. May, S. B. Prusiner, J. Weissman, B. K. Shoichet, *Nat. Chem. Biol.* **2008**, *4*, 197.
- [91] B. Pierkarska, M. Skowronek, J. Rybarska, B. Stopa, I. Roterman, L. Konieczny, *Biochimie* **1996**, *78*, 183.
- [92] M. Skowronek, I. Roterman, L. Konieczny, B. Stopa, J. Rybarska, B. Piekarska, A. Gorecki, M. Krol, *Comput. Chem.* **2000**, *24*, 429.
- [93] P. Spolnik, B. Stopa, B. Piekarska, A. Jagusiak, L. Konieczny, J. Rybarska, M. Krol, I. Roterman, B. Urbanowicz, J. Zieba-Palus, *Chem. Biol. Drug Des.* **2007**, *70*, 491.
- [94] I. H. Cheng, K. Searce-Levie, J. Legleiter, J. J. Palop, H. Gerstein, N. Bien-Ly, J. Puolivali, S. Lesne, K. H. Ashe, P. J. Muchowski, L. Mucke, *J. Biol. Chem.* **2007**, *282*, 23818.
- [95] "Tau Aggregation Inhibitors (TAI) Therapy with Rember™ Arrests Disease Progression in Mild and Moderate Alzheimer's Disease over 50 Weeks" C. M. Wischik, P. Bentham, D. J. Wischik, K. M. Seng, Abstract 03–04–07, International Conference on Alzheimer's Disease, Chicago, **2008**.